PAPER • OPEN ACCESS

Empirical line ratios for optical emission spectroscopy in low-temperature, low-density, magnetised Ar plasmas

To cite this article: Anna Cremona *et al* 2024 *J. Phys. D: Appl. Phys.* **57** 365203

View the article online for updates and enhancements.

Empirical line ratios for optical emission spectroscopy in low-temperature, low-density, magnetised Ar plasmas

Anna Cremona[1,*] , Federica Causa[1] , Andrea Uccello[1] , Daria Ricci[1] ,
Alessandra Giunta[2], Martin O'Mullane[3] and GyM Team[4]

[1] Istituto per la Scienza e Tecnologia dei Plasmi, Consiglio Nazionale delle Ricerche, Milan, Italy
[2] RAL Space, STFC, Rutherford Appleton Laboratory, Harwell Oxford, Didcot, United Kingdom
[3] Department of Physics, University of Strathclyde, Glasgow, United Kingdom

E-mail: anna.cremona@istp.cnr.it

CrossMark

Abstract

Spectroscopic evaluation of electron temperature and density in low-temperature, low-density, magnetized plasmas can be difficult, but necessary in situations where chemical erosion and physical sputtering prevent the use of other diagnostics, such as Langmuir probes (LP). Further, in such cases, because of the low densities and temperatures, the vessel and environment involved, theoretical line ratios derived from Collisional-Radiative models may not be easily applicable. This is the case, for example, of low-temperature (<15 eV), low-density ($<10^{11}$ cm^{-3}), magnetised plasma used for plasma-material interaction studies where chemical erosion and physical sputtering can be significant. The aim of the present work is to define an empirical line ratio (ELR) method derived from an extensive calibration campaign with the two diagnostics, using LP measurements as a reference. The ELR method is useful to permit the use of optical emission spectroscopy independent of LP in conditions that are critical for the latter, resulting in an effective instrument for the evaluation of plasma parameters. Further, the use of two different lines of sight and the influence of the magnetic field intensity on the measurements are also discussed. The proposed ELR method is demonstrated here for pure Ar linear plasmas and is in principle applicable also to other similar cases.

---

[4] See Uccello *et al* 2023 (https://doi.org/10.3389/fphy.2023.1108175) for the GyM Team.
* Author to whom any correspondence should be addressed.

J. Phys. D: Appl. Phys. **57** (2024) 365203

A Cremona *et al*

1. Introduction

The electron temperature (T_e) and electron density (n_e) are important parameters for characterizing low-temperature, low-density, magnetized plasmas in linear machines relevant to plasma wall interaction studies in magnetically confined fusion devices [1], as well as low-pressure plasmas for surface modification of materials in industrial applications [2] and astrophysical plasmas in the solar chromosphere-corona transition region [3]. In laboratory plasmas electron temperature and density are usually derived locally using Langmuir Probes (LPs), which are intrusive and may perturb the plasma. Optical diagnostics, such as optical emission spectroscopy (OES), offer a non-invasive alternative to LP measurements providing extremely powerful insights when supported by an accurate atomic model including metastable states and transport of atoms and ions [4]. OES is particularly useful in experiments aimed at studies of plasma-materials interaction or thin films deposition where the LP tips may be eroded and change their collection area or sputtered material may be deposited on their surface affecting the electrical conductivity.

For the OES diagnostics, a common technique to derive line-of-sight-averaged T_e and n_e from observed spectra consists in using ratios of two emission line intensities which arise from the same atom or ion. The absolute intensity of a spectral line emitted in a transition from level $|j\rangle$ to level $|k\rangle$, I_{jk} [# photons cm^{-3} s^{-1}], defined as:

$$I_{jk} = A_{jk}n_j \tag{1}$$

depends on the spontaneous radiative transition probability (Einstein coefficient) A_{jk} and the population density of the upper excited level n_j, which is established by the interaction between the different species (atoms, ions, free electrons) collectively within the plasma through collisional and radiative processes. The density n_j reflects the key plasma parameters, including T_e and n_e and has to be calculated on the basis of a Collisional-Radiative (CR) model, which consists of a set of rate equations describing the detailed balance between the population and depopulation transitions of the excited states, driven by the competition between collisional and radiative processes [4]. According to the CR model, if the dominant population mechanism of an atomic state $|j\rangle$ is the excitation from the ground state $|g\rangle$ by free electron collisions, the absolute intensity of a spectral line arising from the transition $|j\rangle \rightarrow |k\rangle$ is expressed as [4]:

$$I_{jk} = n_g n_e X_{jk}^{\text{eff}}(n_e, T_e, \ldots) \tag{2}$$

where n_g is the density of atoms on the ground state and $X_{jk}^{\text{eff}}(n_e, T_e, \ldots)$ the effective emission rate coefficient or Excitation Photon Emissivity Coefficient (PEC$^{\text{exc}}$) for that transition:

$$X_{jk}^{\text{eff}}(n_e, T_e, \ldots) \sim A_{jk}\sigma(v_e)v_{egj} = A_{jk}\int_{E_{\text{th}}}^{\infty} \sigma_{gj}(E)(2/m_e)^{1/2}$$
$$\times \sqrt{E}f(E)\,\mathrm{d}E \tag{3}$$

with $\sigma_{gj}(v_e)$ = cross section for an electron impact excitation process from the ground state $|g\rangle$ to the state $|j\rangle$, E_{th} = threshold energy of the excitation process, $f(E)$ = EEDF = Electron Energy Distribution Function (EEDF).

Using lines of the same gas species the direct dependence on n_e and n_g cancels in any line ratio, so that the line intensity ratio is equal to the correspondent PEC$^{\text{exc}}$ ratio, according to this formula:

$$\frac{I_{jk}}{I_{lm}} = \frac{X_{jk}^{\text{eff}}(n_e, T_e, \ldots)}{X_{lm}^{\text{eff}}(n_e, T_e, \ldots)}. \tag{4}$$

In this approach the values of T_e and n_e are derived from the comparison between the observed spectroscopic line ratio and the corresponding theoretical PEC$^{\text{exc}}$ ratio derived from the CR model. Several pairs of lines can be considered in order to compare and average the results. The accuracy of the derived plasma parameters T_e and n_e depends strongly on the quality of the atomic data, such as cross sections and rate coefficients, as well as the number of atomic states considered. This approach requires the knowledge of the theoretical PECs$^{\text{exc}}$. In this context the Atomic Data and Analysis Structure (ADAS) database [5], that is a very powerful instrument for modelling the radiating properties of atoms and ions in astrophysical plasmas and thermonuclear fusion devices, provides the PECs$^{\text{exc}}$, calculated using the population model routine ADAS208 with a Maxwellian EEDF of the free electrons, for all elements up to neon extending to silicon and argon. However, in low-temperature, low-density magnetised laboratory plasma devices a line ratio method [1, 2, 4] relied only on PEC$^{\text{exc}}$ ratios and on the assumption that the ground state is the driving dominant population does not always provide realistic parameters due to the complexity of the atomic processes and particle interactions with the walls. Other processes may be significant such as the excitation from metastable states, recombination processes and radiation trapping phenomena, in addition to non-maxwellian energy distribution functions, magnetic field effects and quenching phenomena. In this framework the present paper proposes an empirical approach to reconstruct emissivity line ratios for Ar^0 and Ar$^+$, based on a calibration procedure of optical spectra with respect to LP measurements, applicable in situations where a suitable theoretical CR model is not available. The proposed approach, referred to as the empirical line ratio (ELR) method, has been developed for a non-contact estimate of plasma parameters, T_e and n_e, in the low-temperature, low-density magnetised plasmas of the linear device Gyrotron Machine (GyM) [6], for plasma-materials interaction experiments in which erosion and sputtering are significant, but may be applicable to other laboratory plasma devices with different configurations. The ELRs-based method is demonstrated here for Ar plasma and, in principle, it is applicabile to other gases or mixtures.

Experimental line emissivity ratios have been determined in relevant GyM operating conditions also for different magnetic fields, with the aim of investigating the effect of magnetic field and providing a valid support for the implementation of an appropriate atomic model describing the plasma of interest.

The ELRs-based method has been validated against LP measurements in linear Ar plasmas in experimental conditions with a negligibile amount of impurities and will be used in scenarios in which the erosion may affect the measurement by the probe.

The paper is structured as follows: the experimental set up is described in section 2; the proposed ELR approach is explained in section 3; the experimental results are presented and discussed in section 4; conclusions are drawn in section 5.

2. Experimental setup

2.1. Linear plasma device

The experimental data discussed here have been acquired in the linear machine GyM [6]. The stainless-steel vacuum chamber (0.25 m diameter, 2.11 m length) is surrounded by ten water-cooled coaxial solenoids carrying the same electric current. The plasma is generated and continuously sustained by a medium-power magnetron source at the electron cyclotron frequency (2.45 GHz), with 3 kW nominal power. The experimental data were taken for Ar plasma in the following operating conditions: 2.5–17.0×10^{-3} Pa pressure, 300–2400 W input power, equivalent to 10%–80% of the nominal source power.

2.2. Diagnostics

The optical emission spectrometer consists of a scanning monochromator (Horiba Jobin Yvon iHR550) of the Czerny–Turner type (focal length = 0.55 m), equipped with a holographic diffraction grating with 1800 grooves mm^{-1}, coupled with a CCD (Synapse Horiba Jobin Yvon) camera, thermoelectrically cooled to -70 °C. The optical emission from the plasma is collected through a UV-grade fused silica viewport using a plane-convex convergent lens of $1''$ diameter and conveyed by an optical fibre (length 5 m, core 600 μm, numerical aperture 0.22) onto the entrance slit of the monochromator (aperture 50 μm). The spectral resolution of the instrument is 0.06 nm and the wavelength accuracy 0.2 nm. The spectroscopic measurements were taken in the sector adjacent to the microwave source along a radial line of sight (LoS1). A second line of sight (LoS2) was used in the same plane but inclined upwards by 30° from a horizontal plane and not intercepting the machine axis (figure 1). The optical system, including optical window and entrance optics, was absolutely calibrated using the OL 455-6S-1 Integrating Sphere Calibration Standard, calibrated for spectral radiance in the 300–900 nm wavelength range.

The Langmuir probe used here is a cylindrical stainless-steel wire protected by a ceramic jacket, with the tip exposed to the plasma. The probe tip of radius $r = 0.75 \times 10^{-3}$ m and length $h = 15 \times 10^{-3}$ m is perpendicular to the magnetic field lines. The probe position is fixed, with the tip placed at 6 cm from the axis of the chamber. The probe current is recorded as the applied voltage is swept with triangular sawtooth bias signal from -67 V to $+74$ V, with 0.01 s period. The plasma is weakly ionised, with ionisation degree of the order
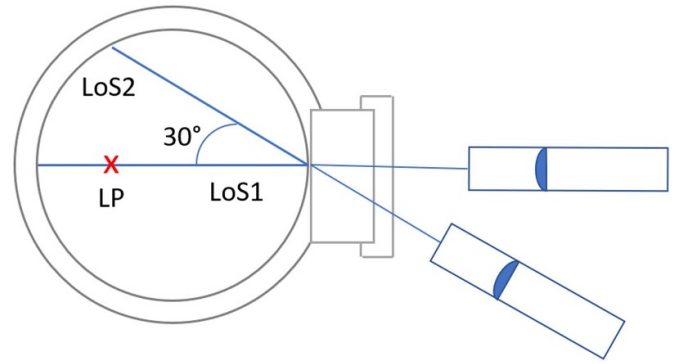
Figure 1. Schematic of the GyM section with the two OES lines of sight (LoS1, LoS2) and the LP position (x).

of a few percent. The operating conditions considered here are such that the ion Larmor radius is larger than the probe radius, which, in turn, is larger than the electron Larmor radius. The ion temperature is assumed to be near room temperature, $T_i \sim 0.05$ eV and, therefore, negligible compared to the electron temperature $T_e \sim 4$–10 eV typically.

## 3. Optical spectra calibration procedure and ELR method

The experimental conditions explored in this work refer to low-temperature, low-pressure, magnetised plasmas. Atomic and molecular models for the interpretation of spectroscopic measurements, in the case of interest for this article, are not readily available or do not reproduce the present experimental data satisfactorily. The comparison of the measured line ratios and the theoretical PEC^{exc} ratios calculated with the ADAS code [5] provides evidence that the experimental data ranges do not intercept the theoretical curves, as it will be shown in section 4 (figures 4 and 6) and consequently the comparison of experimental and calculated line ratios does not permit the estimate of plasma density and temperature. Possible reasons could lie in the complexity of the atomic processes and wall interactions as well as the enhancement of the residence time of the particles in the plasma chamber due to the magnetic field. The discrepancy has been found also in the case of He plasma, as it will be shown in section 4 (figure 7). The experimental observations suggest the need for a more detailed CR model regardless of the accuracy of theoretical atomic data, that might be higher for atoms with low atomic number. In a CR model the rate equation describing the population density n_p of the atom excited state $|p\rangle$ in an optically thin plasma is written as follows:

$$
\frac{dn_p}{dt} = \sum_{q>p} A_{qp} n_q - \sum_{q<p} A_{pq} n_p + n_e \left(\sum_{q \neq p} X_{qp} n_q - \sum_{q \neq p} X_{pq} n_p \right.
$$
$$
\left. + n_g^+ (\alpha_p + \beta_p n_e) - n_p S_p \right) \tag{5}
$$

where X_{qp} are the rate coefficients for excitation from the lower state $|q\rangle$ to the higher state $|p\rangle$ and de-excitation from the higher state $|q\rangle$ to $|p\rangle$ by electron collision, X_{pq} the rate coefficients for excitation from the lower state $|p\rangle$ to the higher state $|q\rangle$ and de-excitation from $|p\rangle$ to $|q\rangle$ by electron collisions, A_{qp} and A_{pq} the transition probabilities for spontaneous emission from and into $|q\rangle$ (Einstein coefficients), α_p and β_p the rate coefficients for radiative and three-body recombination of a positive ion with density n_g^+ ($|g\rangle$ = ground state) into $|p\rangle$ and S_p the rate coefficient for ionization of the state $|p\rangle$. Equation (5) must be extended when other processes, such as collisions with heavy particles, diffusion of metastables with subsequent de-excitation or recombination by collisions with the walls, transport of charged particles in electrostatic and magnetic fields, self-absorption due to the optical thickness, are significant [2, 7, 8]. In addition, a suitable EEDF has to be considered for the calculation of the rate coefficients X_{qp} and X_{pq}. The EEDF is assumed to be Maxwellian in ADAS. In the conditions of interest in GyM, the low-temperature, low-pressure magnetised plasma is generally well described by a Maxwellian EEDF but presents evidence of deviations probably due to interactions with impurities near the walls [9].

The inclusion into the model of terms describing the particle transport in magnetic and electrostatic fields, the neutrals diffusion at a given working pressure and the particles interaction with the walls in a particular geometrical configuration makes the model characteristic for a given plasma discharge or device. Considering the difficulty of modelling these contributions in GyM plasma, especially the strong influence of magnetisation on line ratios, as discussed in section 4.3, an empirical method based on simultaneous measurements by LP and OES is proposed here to calibrate optical spectra and identify suitable line emissivity ratios for the spectroscopic determination of temperature and density. The procedure was applied to Ar spectra where ELRs arisen from neutral Ar^0 or singly ionized Ar^+ lines were chosen for their highest variability (20%–30%) in the operating conditions of interest in terms of pressure and microwave power, as indicated in section 2.1. Measurements with the two diagnostics have been performed also at different values of the magnetic field (specifically, 747 G, 800 G and 880 G corresponding to 560 A, 600 A and 660 A coil currents, reseptively) to investigate possible effects on ELRs due to variations of collisional and radiative excitation and de-excitation processes induced by modifications of the particle dynamics. Then temperature and density values estimated by LP at a distance of 6 cm from the longitudinal axis $\left(T_e^{LP}, n_e^{LP}\right)$ were associated to optical spectra acquired in different experimental conditions. Spectra featured by the the same T_e^{LP} at a given magnetic field were used to reconstruct temperature-dependent ELR curves as a function of n_e^{LP}, assumed as reference density. Similarly, spectra featured by the same n_e^{LP} at a given magnetic field were used to reconstruct density-dependent ELR curves as a function of T_e^{LP}, assumed as reference temperature. Finally, ELRs mainly dependent either on density or temperature were identified to be implemented as instruments for the measurement of the spectroscopic density and temperature, respectively.
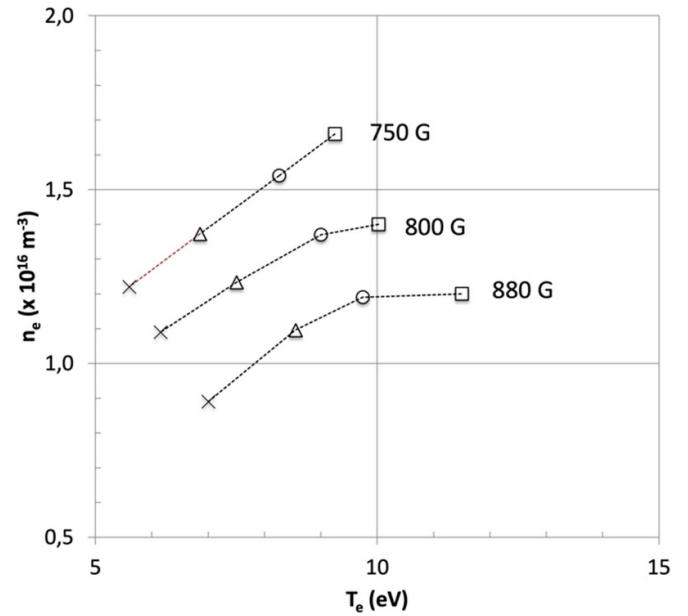

Figure 2. Plasma parameters, T_e and n_e, calculated using the theoretical model at $r = 6$ cm for different values of the applied magnetic field, at different operating pressures [$\times$, Δ, $\bigcirc$, $\square$ = increasing pressure, 0.001, 0.005, 0.01 and 0.02 Pa].

Reliability and accuracy of the proposed methodology were tested experimentally, as discussed in section 4.4.

3.1. Langmuir probe data analysis and modelling

The ELRs have been calibrated using LP data from measurements taken at 6 cm from the machine axis, where plasma parameters are assumed to represent average values along the line of sight. LP data analysis was done following the method described in [9], based on the perimeter sheath expansion method. In the operating conditions of interest here, the ions are weakly magnetised and plasma parameters are extracted from the ion saturation characteristics described by $I = J_s A \left(1 - \exp\left(\frac{V - V_F}{k_B T_e}\right)\right)$, where I is the current, J_s the ion saturation current density, A the probe area, V the probe potential and V_F the floating potential. The model for a positive plasma column in an axial magnetic field described in [10] was used to study the experimental conditions as closely as possible. The plasma model self-consistently solves the momentum and continuity equations to obtain plasma parameters profiles and it was used here to study the effect of the magnetic field on plasma parameters. The low pressures and low ion temperatures provide a low collisionality regime in which electrons are strongly magnetised while ions are weakly magnetised. Results from the model are presented in figure 2, showing the variation of plasma parameters with applied magnetic field, at different operating pressures. These results highlight the complication of the investigated experimental conditions, where the effects of magnetic field and operating pressure may be interchangeable.
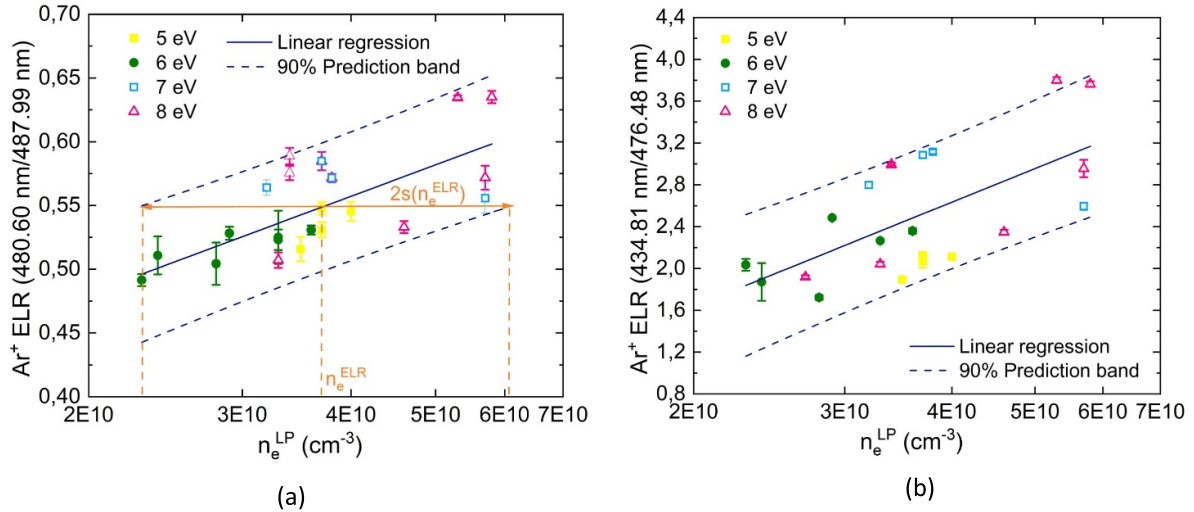
Figure 3. ELRs vs experimental reference density n_e^{LP} (T_e^{LP} = 5–8 eV) for Ar$^+$ (a) 480.60 nm/487.99 nm and (b) 434.81 nm/476.48 nm. Experimental conditions are listed in section 2 (B = 800 G).

4. Experimental results and discussion

Experimental results from dedicated measurements investigating different operating conditions and the effect of magnetic field on the suitably identified ELRs are presented here for Ar plasmas. Considerations on error bar and reliablity of the proposed ELRs-based method, other than measurements along a second OES line of sight (LoS2), are discussed.

The measured absolute line intensities [W cm^{-2} sr^{-1}] have been converted in units of [# photons cm^{-2} s^{-1} sr^{-1}] by the multiplication factor hc/λ. Dividing by the length of the observed plasma and multiplying for the solid angle subtended by the optics, the absolute line intensities could be expressed in units of [# photons cm^{-3} s^{-1}], in coherence with equation (1), but this operation is simplified when intensity line ratios are considered.

In the following, plasma parameters estimated with LP are referred to as n_e^{LP} and T_e^{LP}, considered the reference values and those estimated with the ELR-based method as n_e^{ELR} and T_e^{ELR}.

In the proposed ELR method a linear regression of the experimental points defines the predicted values of n_e^{ELR} or T_e^{ELR} for any given line ratio; the measurement uncertainty $s(n_e^{ELR})$ or $s(T_e^{ELR})$ is defined as the half-width of the 90% prediction band. When more line ratios are used the spectroscopic values n_e^{OES} and T_e^{OES} are determined as the average values from the various line ratios. The method will be discussed in more detail in section 4.1.

### 4.1. Electron density from singly ionised Argon, Ar$^+$

A study addressed to the identification of experimental line ratios with a significant variability (20%–30%) in the range of operability of GyM machine and a dependence on n_e^{LP} or T_e^{LP} mainly was carried out. In the case of Ar plasma two Ar$^+$ line ratios sensitive to density in the region of interest (n_e = 1 × 10^{10}–1 × 10^{11} cm^{-3}) and

only weakly dependent on temperature in the GyM operating conditions (5 eV < T_e < 8 eV) were identified for n_e measurement: 480.60 nm/487.99 nm, already used in [1] and 434.81 nm/476.48 nm, both involving transitions between levels belonging to the multiplets 3s^{2}3p^4(^{3}P)4p–3s^{2}3p^4(^{3}P)4s. The experimental conditions relative to a given magnetic field were divided into groups characterised by the same T_e^{LP} with the purpose of reconstructing temperature-dependent ELR curves as a function of n_e^{LP}. The observed line ratios relative to each T_e^{LP} were plotted in figure 3 as a function of the reference density n_e^{LP}. The temperature-dependent spectroscopic data in the 5–8 eV range measured by LP present an increasing trend vs log $\left(n_e^{LP}\right)$ but it is not possible to distinguish experimental trends associated with individual temperatures. Therefore, all experimental points were used to calculate the linear regression for the predicted values, considering a 90% prediction band. Using the experimental data to determine the spectroscopic density in an experiment, as shown in figure 3(a), a given line ratio corresponds to a predicted n_e^{ELR} determined by linear regression with uncertainty $s(n_e^{ELR})$, defined as the half-width of the density range identified by the prediction band. The uncertainty $s(n_e^{ELR})$ increases as the line ratio increases due to the logarithmic scale on the x-axis.

For a more reliable result it is useful to define the experimental spectroscopic value of the plasma density, n_e^{OES}, at a given operating condition, as the average of ELR-estimates obtained using the two ELRs, 480.60 nm/487.99 nm and 434.81 nm/476.48 nm. An example of n_e^{OES} estimate is presented for different operating conditions in table 1, ordered for decreasing values of n_e^{LP}. The values of n_e evaluated from the two empiric line ratios, n_e^{ELR}, are consistent with each other and their average has been assumed as spectroscopic value of n_e (n_e^{OES}). The ELR/OES results are in agreement with the LP results within the measurement uncertainty and when n_e^{LP} values that differ by less than the uncertainty are considered the ELR trend may be masked by the error bar.

Table 1. Spectroscopic density n_e^{OES} estimated from 480.60 nm/487.99 nm and 434.81 nm/476.48 nm Ar$^+$ ELRs measurements in different operating conditions of GyM machine.

| Operating conditions	T_e^{LP} (eV)	n_e^{LP} ($\times 10^{10}$ cm^{-3})	Line ratio (wavelengths in nm)	n_e^{ELR} ($\times 10^{10}$ cm^{-3})	n_e^{OES} ($\times 10^{10}$ cm^{-3})
2.6×10^3 Pa, 1500 W	7.8	5.7	480.60/487.99: 0.572 434.81/476.48: 2.955	4.6 ± 2.3 5.0 ± 2.6	4.8 ± 2.4
4.9×10^3 Pa, 1200 W	8.9	4.4	480.60/487.99: 0.532 434.81/476.48: 2.891	3.2 ± 1.6 4.8 ± 2.4	4.0 ± 2.0
4.0×10^3 Pa, 1500 W	8.0	3.6	480.60/487.99: 0.527 434.81/476.48: 2.703	3.1 ± 1.4 4.2 ± 2.1	3.7 ± 1.7
8.8×10^3 Pa, 300 W	5.8	2.3	480.60/487.99: 0.496 434.81/476.48: 2.035	2.3 ± 1.1 2.6 ± 1.3	2.4 ± 1.2
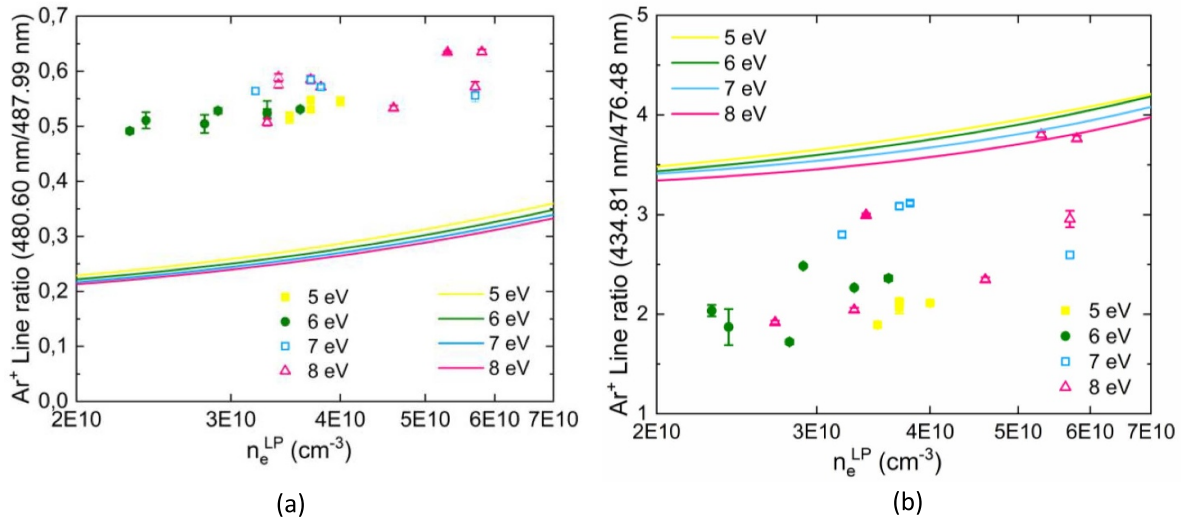
Figure 4. Comparison between ELRs (symbols) vs experimental n_e^{LP} ($T_e^{LP} = 5$–8 eV) and ADAS theoretical PEC^{exc} ratios (solid lines) for Ar$^+$ (a) 480.60 nm/487.99 nm and (b) 434.81 nm/476.48.

The comparison between ELRs vs n_e^{LP} and the theoretical ADAS PEC^{exc} ratios, commonly used in many applications including magnetically confined thermonuclear fusion and astrophysics, for the line ratios 480.60 nm/487.99 nm and 434.81 nm/476.48 nm in the operating conditions of interest is shown in figure 4. These ADAS PEC^{exc} ratios are based on a 452-term R-matrix calculation of electron-impact excitation [5, 11]. Because these data for Ar$^+$ are resolved only by term (nLS), opportune multiplying coefficients proportional to the statistic weights have been applied to derive the PECs^{exc} for the lines corresponding to transitions between (nLSJ) states within the two multiplets $3s^2 3p^4(^3P)4p$ and $3s^2 3p^4(^3P)4 s$ [12]. From the graph it is evident that ADAS curves present an increasing behaviour with density, poorly dependent on temperature, with a significant discrepancy in intensity for both line ratios and also in slope for the line ratio 434.81 nm/476.48 nm, with respect to the experimental data. These observations justify the development of the ELRs-based method to make OES applicable to the experimental conditions of interest.

4.2. Electron temperature from neutral Argon, Ar^0

For the estimate of T_e sixteen Ar^0 lines have been considered and all the possible line ratios $\binom{16}{2} = 120$ between these lines. Among them, twenty-seven line ratios were identified, the ones with the highest variability in the different GyM operative conditions ($B = 800$ G) and closest to ADAS theoretical values. A further choice was made in such a way as to consider only the line ratios that exhibit a clear trend vs the reference temperature T_e^{LP}, without significant dependence on n_e^{LP} in the 3–5×10^{10} cm^{-3} range. From the analysis, the five most suitable ELRs are: 751.47 nm/842.46 nm, 751.47 nm/750.54 nm, 751.47 nm/800.62 nm, 751.47 nm/801.48 nm, 751.47 nm/811.53 nm. The measured values relative to the chosen five ELRs calibrated on LP plasma parameters, T_e^{LP} and n_e^{LP}, are presented in figure 5, where it is seen that in all cases the density-dependent data present an increasing or decreasing behaviour vs T_e^{LP} in the explored temperature range. As a result, using these ELRs to determine the spectroscopic value for temperature, similarly to the procedure illustrated for n_e^{ELR}, a given value of a certain ELR
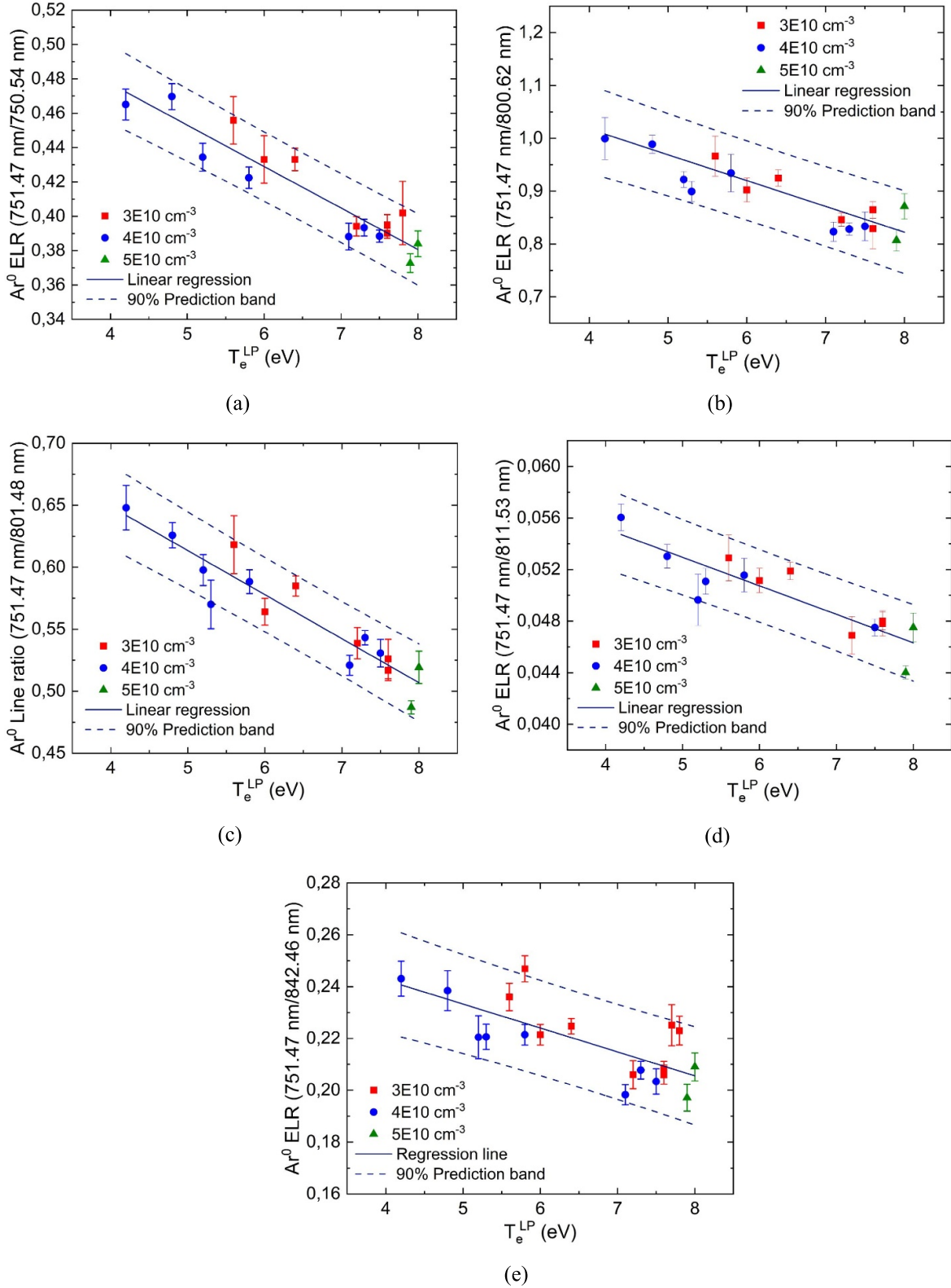
Figure 5. ELRs vs experimental reference temperature T_e^{LP} ($n_e^{LP} = 3$–5×10^{10} cm^{-3}) for Ar^0 (a) 751.47 nm/750.54 nm, (b) 751.47 nm/800.62 nm, (c) 751.47 nm/801.48 nm, (d) 751.47 nm/811.53 nm, (e) 751.47 nm/842.46 nm. Experimental conditions are indicated in section 2.1 ($B = 800$ G).

J. Phys. D: Appl. Phys. **57** (2024) 365203

A Cremona *et al*
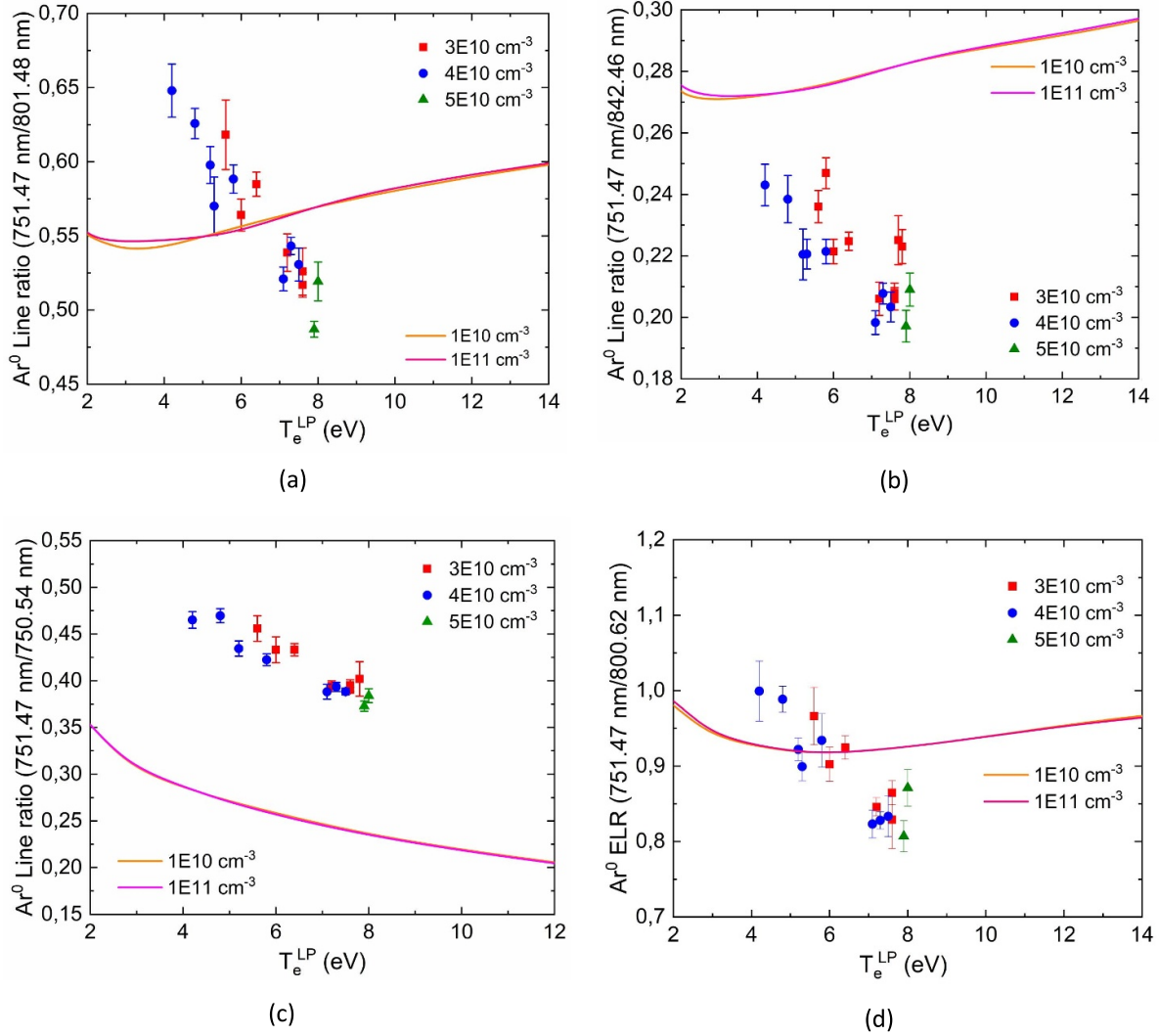
Figure 6. Comparison between ELRs (symbols) vs experimental T_e^{LP} and ADAS theoretical PEC^{exc} ratios (solid lines) for Ar^0 (a) 751.47 nm/801.48 nm, (b) 751.47 nm/842.46 nm, (c) 751.47 nm/750.54 nm and (d) 751.47 nm/800.62 nm in the density range of interest. Experimental conditions are indicated in section 2.1 ($B = 800$ G).

corresponds to a predicted temperature T_e^{ELR}, with uncertainty $s(T_e^{ELR})$ defined using the 90% prediction band. The average on the T_e^{ELR} values from the five lines ratios is assumed as the spectroscopic temperature, T_e^{OES}, at a given operating condition.

The comparison between the measured ELRs and theoretical ADAS PEC^{exc} ratios calculated for the operating conditions of interest is shown in figure 6. The theoretical excitation data for Ar^0 are from R-matrix calculations [13] with radiative transition probabilities from the NIST database [14]. As already mentioned in section 1, it is evident from the graph a discrepancy between the reconstructed density-dependent ELRs and the ADAS curves in the explored experimental conditions.

4.3. ELRs for He^0

The empirical method has been applied also to He line ratios, as mentioned in section 3. He spectroscopic data were associated to T_e^{LP} and n_e^{LP} values and the 667.82 nm/728.13 nm and 396.47 nm/492.19 nm ELRs were plotted vs n_e^{LP} and T_e^{LP} respectively (figure 7). These graphs confirm the discrepancy between experimental and ADAS theoretical data also for He, which is a low-Z gas. A more detailed analysis dedicated to He plasmas will be the subject of future works.

4.4. Magnetic field effects

The effect of the magnetic field on the ELRs has been investigated to better understand the processes responsible for the
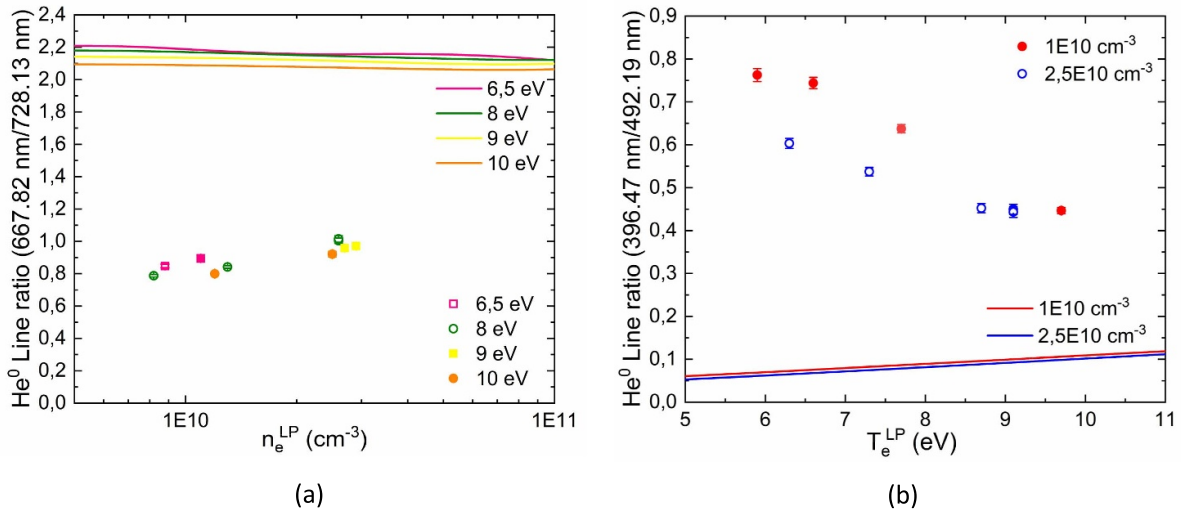
Figure 7. (a) Comparison between He^0 667.82 nm/728.13 nm ELR (symbols) vs experimental n_e^{LP} ($T_e^{LP} = 6.5$–10 eV) and ADAS theoretical PEC^{exc} ratios (solid lines); (b) comparison between He^0 396.47 nm/492.19 nm ELR (symbols) vs experimental T_e^{LP} ($n_e^{LP} = 1$–2.5×10^{10} cm^{-3}) and ADAS theoretical PEC^{exc} ratios (solid lines). [Experimental conditions: $B = 800$ G, pressure = 0.05–0.13 Pa, microwave power = 300–2400 W].
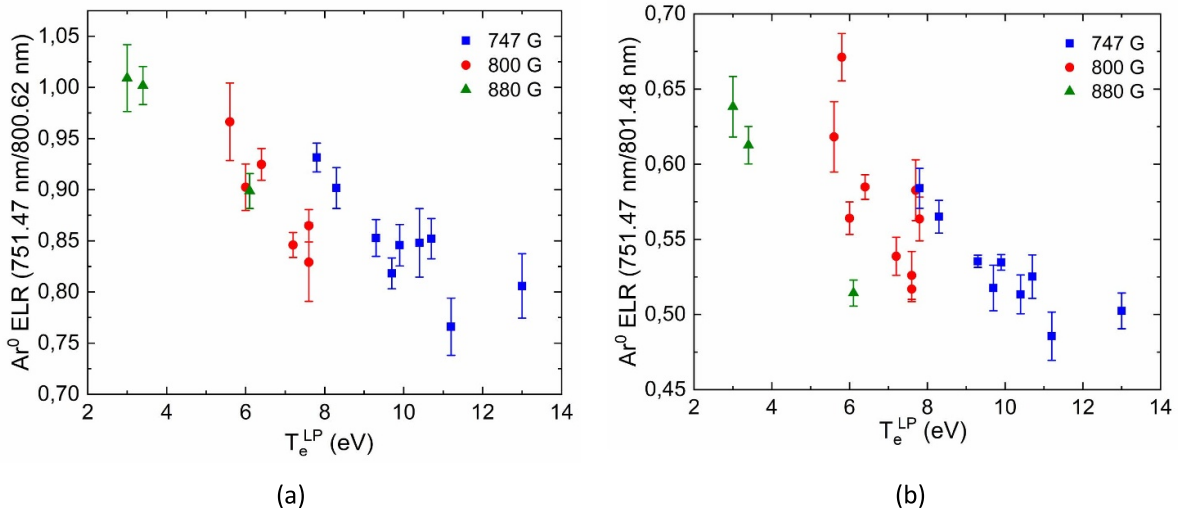
Figure 8. Ar^0 ELRs vs experimental T_e^{LP} at $n_e^{LP} = 3 \times 10^{10}$ cm^{-3} for $B = 747$ G, 800 G, 880 G for (a) 751.47 nm/800.62 nm and (b) 751.47 nm/801.48 nm.

plasma emissivity. Three values of coils current were considered: 560 A, 600 A and 660 A, corresponding to 747 G, 800 G and 880 G, respectively. The ELRs chosen for the temperature measurement were evaluated for the three values of the magnetic field and plotted vs T_e^{LP} at a certain density. An example is given in figure 8. The graphs show that the experimental points move towards lower temperatures as the magnetic field increases in agreement with the simulations presented in figure 2. This means that higher B values at the same temperature and density correspond to lower values of the line emissivity ratios. A possible explanation could be based on the higher confinement time at higher values of B that enhances the collisionality between neutral heavy particles and charged heavy particles giving rise to quenching effects on some atomic transitions and consequently reducing the emissivity of some lines. These results suggest the need to develop a suitable CR model that includes cross-field transport of charged particles (ions and electrons) as well as neutrals transport.

4.5. Reliability testing and validation of the ELR-based method

Reliability and accuracy of the proposed method have been tested experimentally for Ar plasmas in the variability ranges of temperature and density explored in this work. Plasma

J. Phys. D: Appl. Phys. **57** (2024) 365203

A Cremona *et al*

Table 2. Comparison between the values of temperature and density obtained by LP (T_e^{LP}, n_e^{LP}) and ELR-based method (T_e^{OES}, n_e^{OES}) for an Ar plasma in five different operating conditions at B = 800 G.

Operating condition	T_e^{LP}(eV)	T_e^{OES}(eV)	$s(T_e^{OES})/T_e^{OES}$%	n_e^{LP} ($\times 10^{10}$ cm^{-3})	n_e^{OES} ($\times 10^{10}$ cm^{-3})	$s(n_e^{OES})/n_e^{OES}$%
4.9×10^{-3} Pa, 1200 W	8.9	8.3 ± 1.4	17	4.4	4.0 ± 2.0	50
4.8×10^{-3} Pa, 1800 W	8.7	7.7 ± 1.4	18	4.1	4.8 ± 2.5	52
3.5×10^{-3} Pa, 1500 W	8.0	8.5 ± 1.4	16	3.6	3.7 ± 1.7	46
7.8×10^{-3} Pa, 1200 W	5.7	5.7 ± 1.4	25	4.2	3.5 ± 1.6	46
7.7×10^{-3} Pa, 1500 W	5.1	6.0 ± 1.4	23	4.1	3.4 ± 1.7	50

Table 3. Comparison between n_e^{ELR} along LoS1 and LoS2 in three different experimental conditions (800 G).

Operating condition	Line ratio (wavelength in nm)	n_e^{ELR} (LoS1) ($\times 10^{10}$ cm^{-3})	n_e^{ELR} (LoS2) ($\times 10^{10}$ cm^{-3})
3.9×10^{-3} Pa, 1200 W	480.60/487.99	3.5 ± 1.7	2.9 ± 1.5
	434.81/476.48	4.6 ± 2.3	2.9 ± 1.4
1.2×10^{-2} Pa, 600 W	480.60/487.99	2.2 ± 1.1	1.9 ± 1.0
	434.81/476.48	2.7 ± 1.3	2.0 ± 0.9
1.3×10^{-2} Pa, 1200 W	480.60/487.99	2.3 ± 1.2	1.9 ± 1.5
	434.81/476.48	2.6 ± 1.2	1.7 ± 0.8

parameters estimated during an impurity-free experimental campaign in Ar plasma using the ELRs drawn in figures 3 and 5 were compared in table 2 with the ones determined by LP. The two estimates are in good agreement, within 20%. The table is ordered for LP decreasing temperatures. The OES trend in temperature between measurements in the different operating conditions is coherent to the LP trend if measurements corresponding to values of T_e^{LP} that differ by more than 1 eV are considered, for example the measurements corresponding to 8.0 eV and 5.7 eV. If too close values of T_e^{LP} are considered, the ELR trend can be masked by the error bars. Anyway, the accordance between ELR method and LP diagnostics is in the range of the estimated errors. Similar considerations apply to density measurements as discussed in section 4.1.

4.6. Comparison of spectroscopic measurements along LoS1 and LoS2

To test and verify the ELR-based method, optical spectra have been acquired also along LoS2, the line of sight shown schematically in figure 1, that does not intercept the axis of the plasma column. This is a useful test because in the operating conditions of interest the temperature is expected to remain almost unchanged, while the density is expected to be significantly reduced in the outer regions of the plasma [10]. Measurements were carried out in ten different operating conditions. In all investigated conditions the line ratios identified for temperature measurement do not present significant variations along the two lines of sight and

consequently the corresponding values of T_e obtained from ELRs in figure 5 are quite the same. This result is consistent with the simulations from the plasma model presented in [10]. Concerning the density measurement, 480.60 nm/487.99 nm ELR shows a percentage variation between LoS1 and LoS2 <20% while 434.81 nm/476.48 nm ELR presents higher variations up to 40%, corresponding to lower density values along LoS2. Experimental values obtained in three different operating conditions are presented in table 3 to show that 434.81 nm/476.48 nm ELR, due to its higher slope, is more sensitive to density changes than 480.60 nm/487.99 nm. The lower values of n_e derived from 434.81 nm/476.48 nm ELR, due to the greater extension of LoS2 in the outer regions of the plasma column, are in accordance with the density profile measured by LP [10]. The measurements are also coherent when compared in the different operating conditions.

5. Conclusion

Empiric line emissivity ratios ELRs have been determined for the spectroscopic determination of T_e and n_e in low-temperature, low-density, magnetised plasmas, especially in scenarios dedicated to plasma-material interaction studies, where chemical erosion and physical sputtering affect Langmuir electrostatic probe measurements. The proposed method is demonstrated here for pure Ar and outlined for He, but in principle may be applicable also to other cases.

The experimental line ratios have been calibrated in temperature and density using the LP data acquired in a position

J. Phys. D: Appl. Phys. **57** (2024) 365203

A Cremona *et al*

that represents the average values of T_e and n_e along the line of sight. Line ratios depending mainly on T_e or n_e have been identified for Ar plasma in such a way to perform independent measurements of temperature and density. The temperature and density trends of ELRs resemble the ADAS theoretical curves but provide different experimental ranges of the spectroscopic line ratios corresponding to plasma parameters in abscissa assumed as reference parameters for the experimental conditions of interest.

In the proposed ELR method a linear regression of the experimental points defines the predicted values of n_e^{ELR} or T_e^{ELR} for any given line ratio; the measurement uncertainty $s(n_e^{\text{ELR}})$ or $s(T_e^{\text{ELR}})$ is defined as the half-width of the range corresponding to the 90% prediction band. Different line ratios can be considered and the average n_e^{ELR} or T_e^{ELR} is assumed as spectroscopic value n_e^{OES} or T_e^{OES}.

The ELR method has been validated against LP during an impurity-free experimental campaign in Ar plasma. The measurements have shown that ELR/OES method and LP diagnostics are in the case of interest in good agreement within the range of the estimated error (of the order 1×10^{10} cm^{-3} for density and 1 eV for temperature).

The ELRs given as a function of temperature or density are characteristic of GyM machine and depend on geometry, pressure, magnetic field and plasma source but the proposed method may be implemented in other experimental environments where there is a reference diagnostics (LP in the case discussed here). Thereby, ELRs characteristic of a particular reactor can be derived and applied to scenarios where LP or other diagnostics cannot be used.

Data availability statement

The data cannot be made publicly available upon publication because no suitable repository exists for hosting data in this field of study. The data that support the findings of this study are available upon reasonable request from the authors.

Acknowledgments

ORCID iDs

Anna Cremona https://orcid.org/0000-0001-8207-8597
Federica Causa https://orcid.org/0000-0003-0508-3100
Andrea Uccello https://orcid.org/0000-0003-3044-1715
Daria Ricci https://orcid.org/0000-0001-8794-4909
Martin O'Mullane https://orcid.org/0000-0002-2160-4546

References

[1] Fantz U, Falter H, Franzen P, Wünderlich D, Berger M, Lorenz A, Kraus W, McNeely P, Riedl R and Speth E 2006 *Nucl. Fusion* **46** S297
[2] Siepa S, Danko S, Tsankov T V, Mussenbrock T and Czarnetzki U 2014 *J. Phys. D: Appl. Phys.* **47** 445201
[3] Giunta A S, Fludra A, Lanzafame A C, O'Mullane M G, Summers H P and Curdt W 2005 *Astrophys. J.* **803** 66
[4] Fantz U 2006 *Plasma Sources Sci. Technol.* **15** S137
[5] Summers H and O'Mullane M 2020 OPEN-ADAS *ADF15 - Photon emissivity coefficients* (available at: https://open.adas.ac.uk)
[6] Uccello A *et al* 2023 *Front. Phys.* **11** 1108175
[7] Zhu X M and Pu Y K 2010 *J. Phys. D: Appl. Phys.* **43** 403001
[8] Bogaerts A, Gijbels R and Vlček J 1998 *J. Appl. Phys.* **84** 121
[9] Causa F, Gervasini G, Uccello A, Granucci G, Ricci D and Rispoli N 2021 *Plasma Sources Sci. Technol.* **30** 045008
[10] Causa F, Gittini G, Minelli D, Mellera V, Uccello A, Nardone A and Ripamonti F 2022 *Plasma Sources Sci. Technol.* **31** 075007
[11] Griffin D C, Balance C P, Loch S D and Pindzola M S 2007 *J. Phys. B* **40** 4537
[12] Condon E U and Shortley G H 1959 *The Theory of Atomic Spectra* (Cambridge University Press) ch 9
[13] Balance C P 2015 private communication
[14] Kramida A , Ralchenko Yu and Reader J 2023 *NIST Atomic Spectra Database Lines Data* (available at: www.nist.gov/pml/atomic-spectra-database)